frontiers in Animal Science

TYPE Original Research
PUBLISHED 08 May 2026
DOI 10.3389/fanim.2026.1763451

OPEN ACCESS

EDITED BY
Francisco Javier Navas González,
University of Cordoba, Spain

REVIEWED BY
Simara Larissa Fanalli,
University of São Paulo, Brazil
Drahomira Ctvrtlikova Knitlova,
Mendel University in Brno, Czechia

*CORRESPONDENCE
Maria Ballester
maria.ballester@irta.cat
Josep M. Folch
josepmaria.folch@uab.es

RECEIVED 08 December 2025
REVISED 02 March 2026
ACCEPTED 09 March 2026
PUBLISHED 08 May 2026

CITATION
Liu J, Vourlaki I-T, Sebastià C, Llobet-Cabau F, Sánchez A, Castelló A, Ramayo-Caldas Y, Ballester M and Folch JM (2026) Identification of plasma fatty acids as biomarkers for carcass traits and tissue-specific fatty acids profile in pigs.
Front. Anim. Sci. 7:1763451.
doi: 10.3389/fanim.2026.1763451

Identification of plasma fatty acids as biomarkers for carcass traits and tissue-specific fatty acids profile in pigs

Junhui Liu[1,2], Ioanna-Theoni Vourlaki[3], Cristina Sebastià[1,2], Ferran Llobet-Cabau[1,2], Armand Sánchez[1,2], Anna Castelló[1,2], Yuliaxis Ramayo-Caldas[3], Maria Ballester[3]* and Josep M. Folch[1,2]*

[1]Plant and Animal Genomics, Centre for Research in Agricultural Genomics (CRAG), CSIC-IRTA-UAB-UB Consortium, Bellaterra, Spain, [2]Departament de Ciència Animal i dels Aliments, Facultat de Veterinària, Universitat Autònoma de Barcelona (UAB), Bellaterra, Spain, [3]Animal Breeding and Genetics Program, Institut de Recerca i Tecnologia Agroalimentàries (IRTA), Caldes de Montbui, Spain

Carcass and pork traits have long been regarded as key phenotypes in pig breeding. The content and composition of fatty acids (FAs) play a crucial role in determining carcass and meat quality in pigs, as their regulation affects fat depositions. The current study integrates the FA composition of blood, liver, backfat and muscle, and explores its relationship with carcass traits in 265 commercial Duroc pigs. In muscle, higher levels of C16:0 and C18:1*n*-9 were positively correlated with carcass weight (CW) and fat thickness in backfat (BFT34) and ham (HFT), but negatively correlated with lean percentages. Conversely, PUFA levels in muscle showed the opposite correlation pattern. Backfat FAs like C16:0, C18:0, C20:0, and C20:1*n*-9 were positively correlated with CW, BFT34, and HFT, while also negatively correlated with lean meat percentage (LM). Liver FAs such as C16:0, C18:0, and C18:1*n*-7 exhibited similar correlation patterns with CW, BFT34, HFT, and LM. Blood FAs showed a different correlation pattern compared to the other tissues, with MUFA and C18:2*n*-6 positively correlated with CW, BFT34 and HFT, while the levels of C16:0, C16:1*n*-7, C18:1*n*-9, and C18:2*n*-6 in blood showed a negative correlation with LM. Inter-tissue communication revealed positive correlations between C16:0, C16:1*n*-7, C18:1*n*-7, and C18:1*n*-9. Additionally, the PUFA content in muscle was inversely related to FAs from other tissues. In Duroc pigs, during the early growth stage, there is a positive correlation among the levels of C16:0, C16:1*n*-7, C18:1*n*-7, and C18:1*n*-9 FAs in the blood, which is reflected in their concentrations within the liver, backfat, and muscle tissues after pig slaughter. Moreover, these FAs showed a positive correlation with CW and BFT34 and HFT, and were negatively correlated with LM. Among these FAs, C16:0 and C18:0 as well as the desaturation product C18:1*n*-9, along with C18:2*n*-6, exhibited great predictive ability in muscle FAs and less ability in carcass traits. In conclusion, the plasma C16:0, C16:1*n*-7 C18:0, C18:1*n*-9 and C18:2*n*-6 are proposed as the main candidate indicators for predicting carcass traits in slaughtered pigs and the FA profile in liver, backfat and muscle.

KEYWORDS
carcass traits, correlation, fatty acid, pig, predictor

1 Introduction

Pork is one of the main meats consumed by people, offering essential energy and nutrition to the body. Meat quality attributes such as flavor, color, marbling score, and tenderness are pivotal factors influencing consumer preferences, which can be affected by lipid deposition and composition (Yi et al., 2023). For instance, the marbling score reflects intramuscular fat (IMF) which represents the visible fat distributed within muscle fibers alongside lean meat, and which is deposited mainly in the later stages of growth (Malgwi et al., 2022; Wood et al., 1999). When the energy is provided by feed over the energy needed for muscle deposition, it leads to an increase in the concentration of IMF and meat tenderness (Wood et al., 1999).

In addition to the association of FA with meat quality, the structure and composition of FA have health effects on human organisms. FAs are classified into saturated fatty acids (SFA), monounsaturated fatty acids (MUFA), and polyunsaturated fatty acids (PUFA). Some SFA can affect the ability of plasma lipoproteins to carry cholesterol, leading to a high risk of cardiovascular diseases, while PUFA contributes to reducing the risk of diabetes (Dooley and Ryan, 2019). The latest advances in the link between FAs and immunity focus on FA regulation in adaptive immunity. Lim et al (Lim et al., 2022). reviewed that lipid metabolism is a key regulator for T cell biology, which orchestrates adaptive immunity, and the dysfunction of T cells leads to cancer pathogenesis and autoimmunity. The activated T cells promote the *de novo* FAs synthesis, where the enzymes acetyl-CoA citrate lyase (*ACLY*), acetyl-CoA carboxylase 1 (*ACC1*), and fatty acid synthase (*FASN*) are involved (Lim et al., 2022). The differentiation of inducible regulatory T (iTreg) cells from activated T (Th0) cells with the metabolism shift from FA synthesis to FA oxidation (FAO) and accompanied by the ubiquitination and degradation of ACLY (Tian et al., 2021). Therefore, the FAs reprogramming is critical for maintaining homeostasis with the emergence of pathogens or changes in the environment.

Adipose tissue, muscle and liver are the three main organs that store fat. These stored fats can undergo hydrolysis through a regulated pathway to release FA (Frayn et al., 2006). The origin of FA comprises both endogenous synthesis and exogenous sources from dietary intake. The aerobic oxidation of carbohydrates, beta-oxidation of FAs, and amino acids catabolism generate the intracellular acetyl-CoA that is the substrate for *de novo* synthesis of endogenous FAs. Dietary fat enters the bloodstream from the small intestine and is packaged into the chylomicrons. Lipoprotein lipase, which is bound to the endothelial cells lining the capillaries of adipose tissues and muscle, can enzymatically hydrolyze the triacylglycerol releasing FAs (Frayn et al., 2006). In the meantime, the non-esterified FAs (NEFA) are released from adipose tissue into the plasma and are subsequently taken up by muscle and liver tissues. In addition, when FA synthesis exceeds degradation, it results in fat accumulation, with the deposited FA within the cell serving as an energy source (Yi et al., 2023). Adipose tissue will enhance fat mobilization to support the energy needs of skeletal muscle during physical activity. In summary, FA metabolism involves the participation of multiple tissues, with collaboration among them. Therefore, determining and regulating the FA composition of meat is important.

Plasma triglycerides (TAG) and cholesterol are well-known predictors of cardiovascular events (Fernandez et al., 2013). However, the plasma lipidome is complex, consisting of hundreds of individual lipid species. Consequently, accurately and consistently assessing many metabolites for the purpose of discovering biomarkers remains a significant challenge (Stegemann et al., 2014). Studies reported blood lipid profiles are reliable biomarkers of dietary intake, being this particularly evident for fatty acids with limited endogenous synthesis, such as PUFA n-3, n-6, and trans fatty acids. and plasma phospholipid FA profiles (Hodson et al., 2008; Liu et al., 2019; Saadatian-Elahi et al., 2009). Senanayake et al. (2014) observed that a dietary substitution of 10% of total energy from PUFA n-6 with PUFA n-3 results in a corresponding 2–3% substitution in plasma. Warensjö et al (Warensjö et al., 2005). suggested that FA composition in serum may serve as a predictor for the long-term development of the metabolic syndrome. Additionally, not only the FA composition of serum but also that in plasma is used to predict the risk of future disease, providing valuable insights into mechanisms of disease pathogenesis, and identify lipid biomarkers of risk (Anderson et al., 2009; Bajerska et al., 2023).

Nevertheless, the discovery of biomarkers requires looking for associations in a variety of data. In the past decade, data integration methods have become increasingly popular. Integrative approaches can work together with multiple types of biological data and provide more comprehensive, systems-level biological insights (Gligorijević and Pržulj, 2015). The development of data integration approaches, particularly DIABLO, a strategy for data integration analysis and biomarker discovery using latent components, aims to identify common information across different datasets as well as discriminate between multiple phenotypic groups (Singh et al., 2019).

The broad objective of this work was to describe the relationships among the FA composition of blood, liver, backfat, and muscle in pigs using data integration approaches. The final aim was to identify plasma FA biomarkers of the early fattening process as a strategy for predicting the FA profiles in adipose tissue, muscle, and liver at slaughter.

2 Methods

2.1 Animal material

The study employed a total of 265 commercial Duroc pigs, consisting of 136 males and 129 females. All pigs were reared under uniform conditions with *ad libitum* access to a cereal-based diet and water. The ingredient and nutrient composition of diets are shown in Supplementary Table 1. Blood samples were obtained from the jugular vein when the pigs were 60 ± 8 days old, with body weights of 18.76 ± 2.80 kg. Subsequently, the animals were slaughtered at an age range of 181 to 228 days in a commercial abattoir. Immediately after slaughter, samples of adipose tissue (backfat), liver (inner part

of the left lateral lobe), and *gluteus medius* muscle were collected and promptly frozen at -80 °C for further analysis.

2.2 Fatty acids measurement

FAs were detected and measured using gas chromatography (GC) of methyl esters (FAMEs). The plasma FAs were analyzed at the IRBLleida Lipidomics Core Facility – PLICAT following previously described methods (Jové et al., 2021). In summary, 10 µl of plasma were used for FAMEs extraction and separation was carried out using a DBWAX capillary column (30 m × 0.25 mm × 0.20 µm) in a GC System 7890A equipped with a Series Injector 7683B and an FID detector (Agilent Technologies, Barcelona, Spain). The FAMEs were identified by comparison with authentic standards (Larodan Fine Chemicals, Malmö, Sweden). FA composition of liver, backfat (taken between the third and fourth last ribs) and *gluteus medius* muscle samples was analyzed in the NUTRICAL-UCM laboratory. The procedure of extraction and methylation with samples was described by Segura and Lopez-Bote (Segura and Lopez-Bote, 2014). FAMEs were identified and quantified by GC (6890 Hewlett Packard, Avondale, PA, USA), using a capillary column (HP- Innowax, 30 m x 0.32 mm id and 0.25 µm cross-linked polyethylene glycol) (Agilent Technologies GmbH, Wald-bronn, Germany) and standards (Sigma-Aldrich, Tres Cantos, Madrid, Spain). The concentrations of FAs were expressed as a percentage relative to the total FAs present in the sample.

2.3 Carcass traits determination

The determination of carcass traits has been described by (Jové-Juncà et al., 2024). After slaughter, the carcass weight (CW, kg) was measured. Using an online ultrasound automatic scanner (AutoFOM, Frontmatec Group, Kolding, Denmark), the carcass lean meat percentage (LM) and the lean meat percentage of the main retail cuts, including ham (HLM), loin (LLM), and shoulder (SLM) were estimated. The LM was determined using measurements with 16 ultrasonic transducers, which conducted scans of the carcass every 5 mm. Additionally, these transducers estimated the backfat thickness (BFT34) and loin thickness (LD34) at 6 cm from the midline between the third and fourth last ribs, as well as fat thickness in the ham (HFT).

2.4 Data preparation

Descriptive statistics were performed for each trait. The raw data has been transformed with centered log-ratio followed by the correction of sex and batch, which is the environmental seasonal and farm effects. Additionally, carcass traits raw data was corrected by age (days) at slaughter.

2.5 Bioinformatic analysis

Two analyses were performed with different grouping methods. For the grouping, a principal components analysis (PCA) was performed with carcass traits and the first principal component score was selected as the carcass traits score. Animals were classified into high, medium, and low groups according to the carcass traits score.

The DIABLO bioinformatic approach of *mixomics* (version 6.32.0) package (Rohart et al., 2017) was employed in R (version 4.3.1) to integrate the FA datasets from different tissues. The analysis was performed with *block.plsda* function and the design matrix with the minimal link of 0.1. The number of the components was determined by *Mfold* validation methods with the *perf* function. Additionally, the same validation method was used for feature selection by *tune* function. The network generated was based on the *Diablo* analysis and only correlations higher than 0.6 or lower than -0.6 were exported to Cytoscape (version 3.10.4) and generated relevance network plot (Shannon et al., 2003). Data preprocessing and visualization were performed using the ggrepel (version 4.5.0), ggplot2 (version 3.5.2),dplyr (version 1.1.4) and tidyverse (version 2.0.0).

2.6 Prediction

Prediction was performed using the BayesC method from the BGLR package (version 1.1.4) (Pérez and De Los Campos, 2014). BayesC is a Bayesian regression approach that combines variable selection with shrinkage of the estimated effects. Specifically, it assumes that a proportion of the predictor variables have no effect, allowing for sparse solutions. This makes BayesC particularly suitable for scenarios with a relatively small number of predictors, where incorporating prior assumptions is desirable. In this study, BayesC was used to assess the predictive ability of blood-derived fatty acids across seven traits independently and robustly. In BayesC, the probability that a marker has a non-zero effect is modelled using a Beta prior distribution $\pi \sim Beta\ (a = \pi_0 \cdot p_0, \beta = (1 - \pi_0) \cdot p_0)$ where π_0 is the prior expected inclusion probability, and p_0 is the total number of prior counts (i.e., the sum of prior successes and failures), reflecting the strength of the prior belief. Each marker effect β_j is therefore non-zero with probability π, and zero with probability $1 - \pi$. For this analysis, two prior inclusion probabilities were tested: π_0=0.01 and π_0=0.25, with p_0=5. The model used can be described as (Equation 1):

$$\mathbf{y} = \mu + X\beta + e, \quad (1)$$

where y is the $n \times 1$ vector of phenotypic values (with n being the number of individuals) for each of the seven traits: CW, LM, LLM, BFT34, C16:0, C18:1*n*-9, and C18:2*n*-6 in muscle. μ is the overall mean, β is the vector of marker effects, and X is the $n \times N_{BL}$ matrix of standardized blood fatty acid predictors. As a baseline analysis, we implemented the BayesC model using all 19 available blood-derived fatty acids to evaluate their collective predictive ability for the target traits. Subsequently, model (1) was fitted again using a reduced subset of four selected FAs in blood (C16:0, C18:0, C18:1*n*-9, and C18:2*n*-6) to assess whether this smaller predictor set could retain sufficient predictive power. The reduced subset of four FAs was selected based on their consistently large, estimated effects obtained from initial analyses using the full set of 19 predictors within the training data partitions. This selection aimed to focus on the most informative markers for each training fold while avoiding overfitting.

For each trait, we implemented a 5-fold cross-validation procedure repeated three times, resulting in a total of 15 training/testing partitions per trait. Models were trained on each training set and evaluated on the corresponding test set using the Pearson correlation coefficient as the performance metric. BGLR was run for 100,000 iterations, using the first 500 iterations as burn-in and thinning interval of 5. Convergence plots of the residual variance from the BayesC models are provided in Supplementary Figures 1, 2.

3 Results

3.1 Descriptive statistics for fatty acid composition and carcass traits in Duroc pigs

Tables 1, 2 summarize the descriptive statistics for carcass traits and FA traits in 265 Duroc pigs. In total, twenty-five FAs were measured, but there were differences in the FAs measured in each tissue. Nineteen FAs were detected in plasma, 20 FAs in liver, 18 FAs in backfat, and 22 FAs in muscle. The most abundant FAs were C18:2*n*-6 in plasma, C18:0 in liver, and C18:1*n*-9 in backfat and muscle. Eight carcass traits have been measured, with the LLM exhibiting the highest variation (CV = 0.28).

3.2 Principal component analysis with carcass traits and muscle fatty acids

Principal component analysis (PCA) was performed with carcass traits (Figure 1A) and muscle FAs (Figure 1B). The component matrices of carcass traits and muscle FAs are shown in Supplementary Tables 2, 3, respectively. The first component (PC1) of carcass traits described 74.7% of the variance of the original dataset and separated pigs with high LM (and other related lean meat measures like HLM, LLM and SLM) from animals with high BFT34 (and the related HFT) and high CW. For muscle FAs, the PC1 explained 87.9% of the variance of the row dataset and differentiated animals with high C18:2*n*-6 content from pigs with high C18:1*n*-9 and C16:0 percentages in muscle.

TABLE 1 Descriptive statistics summary for fatty acid composition in Duroc pigs.

Trait	Name	Blood			Liver			Backfat			Muscle		
		Mean	SD	CV	Mean	SD	CV	Mean	SD	CV	Mean	SD	CV
C14:0	Myristic acid	1.06	0.56	0.53	0.61	0.26	0.43	1.39	0.13	0.09	1.60	0.24	0.15
C16:0	Palmitic acid	20.42	1.43	0.07	22.50	2.15	0.10	24.34	1.14	0.05	23.13	3.00	0.13
C18:0	Stearic acid	15.10	1.51	0.10	30.72	5.16	0.17	13.22	1.48	0.11	11.52	1.49	0.13
C20:0	Arachidic acid	–			0.24	0.11	0.45	0.20	0.03	0.16	0.15	0.05	0.35
C22:0	Behenic acid	0.22	0.10	0.44	–			–			–		
C24:0	Lignoceric acid	0.81	0.17	0.21	–			–			–		
C16:1n-7	Palmitoleic acid	0.58	0.12	0.20	1.12	0.40	0.36	2.05	0.31	0.15	2.74	0.57	0.21
C18:1n-7	Vaccenic acid	1.91	0.37	0.19	2.31	0.30	0.13	2.59	0.33	0.13	3.68	0.72	0.20
C18:1n-9	Oleic acid	14.82	1.94	0.13	21.71	3.89	0.18	41.87	2.27	0.05	39.12	4.89	0.12
C20:1n-9	Gondoic acid	0.28	0.11	0.40	0.27	0.06	0.21	0.89	0.11	0.12	0.60	0.13	0.21
C22:1n-9	Erucic acid	1.28	2.05	1.61	–			0.10	0.05	0.47	0.08	0.11	1.38
C24:1n-9	Nervonic acid	0.55	0.15	0.27	0.46	0.22	0.47	–			0.08	0.08	1.01
C18:3n-3	Alpha-Linolenic acid	0.47	0.20	0.43	0.25	0.11	0.44	0.69	0.09	0.13	0.40	0.08	0.19
C18:4n-3	Stearidonic acid	–			0.09	0.04	0.46	0.07	0.01	0.20	0.06	0.01	0.21
C20:3n-3	Eicosatrienoic acid	–			–			0.12	0.02	0.12	0.07	0.02	0.32
C20:5n-3	Eicosapentaenoic acid	0.49	0.13	0.27	0.32	0.33	1.04	–			0.07	0.06	0.85
C22:5n-3	Clupanodonic acid	–			0.44	0.23	0.53	0.06	0.02	0.26	0.31	0.21	0.70
C22:6n-3	Docosahexaenoic acid	1.09	0.26	0.24	0.45	0.24	0.53	–			0.10	0.08	0.81
C18:2n-6	Linoleic acid	33.30	3.51	0.11	11.22	2.41	0.21	11.45	1.66	0.14	12.55	4.76	0.38
C18:3n-6	Gamma linolenic acid	–			0.11	0.06	0.59	–			0.07	0.05	0.66
C20:2n-6	Eicosadienoic acid	0.30	0.12	0.40	0.40	0.09	0.22	0.60	0.07	0.12	0.42	0.08	0.20
C20:3n-6	Dihomo-γ-linolenic acid	0.45	0.14	0.31	0.36	0.16	0.44	0.08	0.01	0.18	0.35	0.23	0.66
C20:4n-6	Arachidonic acid	6.46	1.17	0.18	6.03	2.37	0.39	0.16	0.03	0.17	2.56	1.87	0.73
C22:4n-6	Adrenic acid	–			0.42	0.23	0.56	0.11	0.03	0.25	0.32	0.21	0.66
C22:5n-6	Osbond acid	0.40	0.16	0.40	–			–			–		

10.3389/fanim.2026.1763451

TABLE 2 Descriptive statistics summary for carcass traits in Duroc pigs.

Trait	Name	Mean	SD	CV
CW	Carcass weight (kg)	99.06	11.46	0.12
LM	Lean meat percentage (%)	40.27	6.52	0.16
HLM	Ham lean meat percentage (%)	59.45	6.09	0.10
LLM	Loin lean meat percentage (%)	36.91	10.24	0.28
SLM	Shoulder lean meat percentage (%)	54.90	5.84	0.11
BFT34	Backfat thickness at 3rd–4th rib (mm)	31.22	6.68	0.21
LD34	Loin thickness at 3rd–4th rib (mm)	45.83	6.23	0.14
HFT	Ham fat thickness (mm)	20.78	4.44	0.21

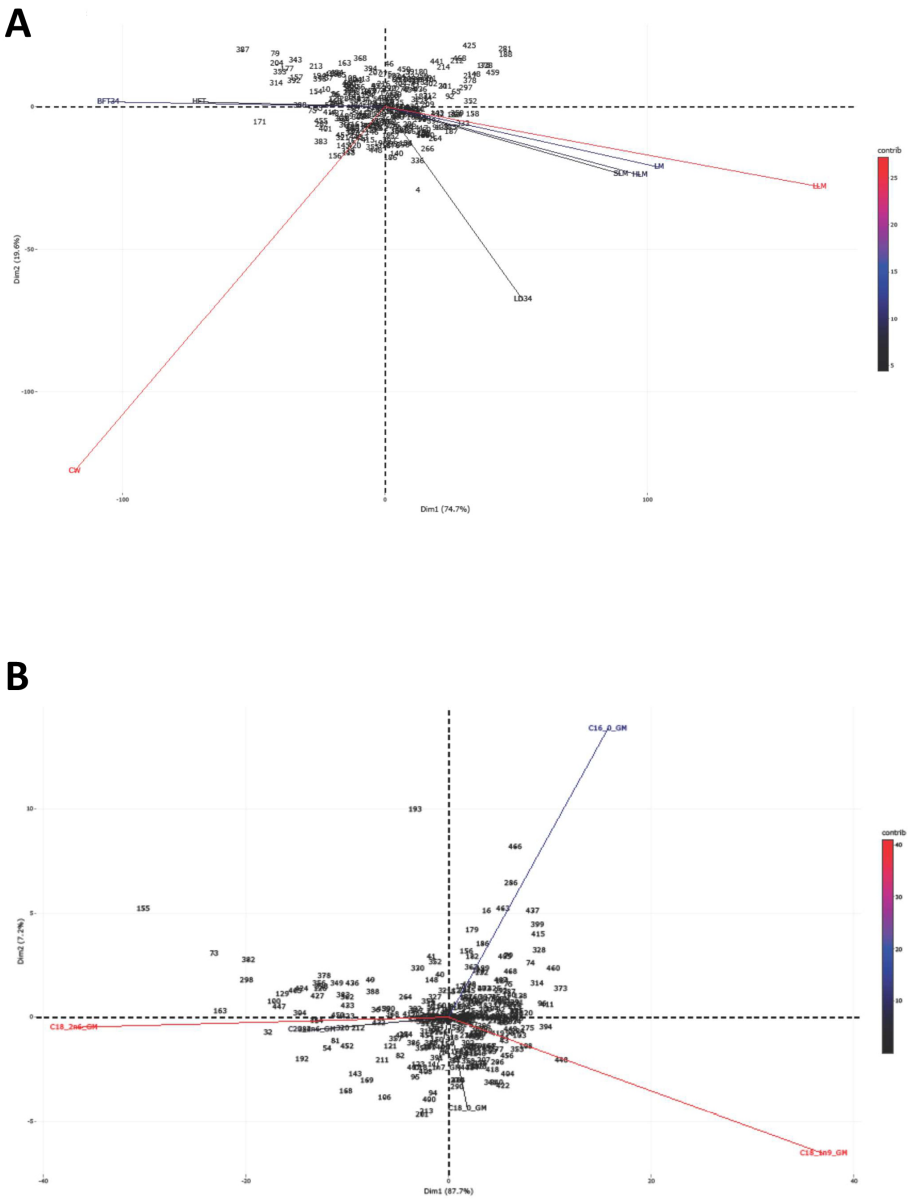

FIGURE 1
Principal components analysis with **(A)** carcass traits and **(B)** muscle fatty acid composition. CW, carcass weight; HLM, ham lean meat percentage; LLM, loin lean meat percentage; SLM, shoulder lean meat percentage; BFT34, backfat thickness; HFT, ham fat thickness; GM, gluteus medius muscle.

10.3389/fanim.2026.1763451

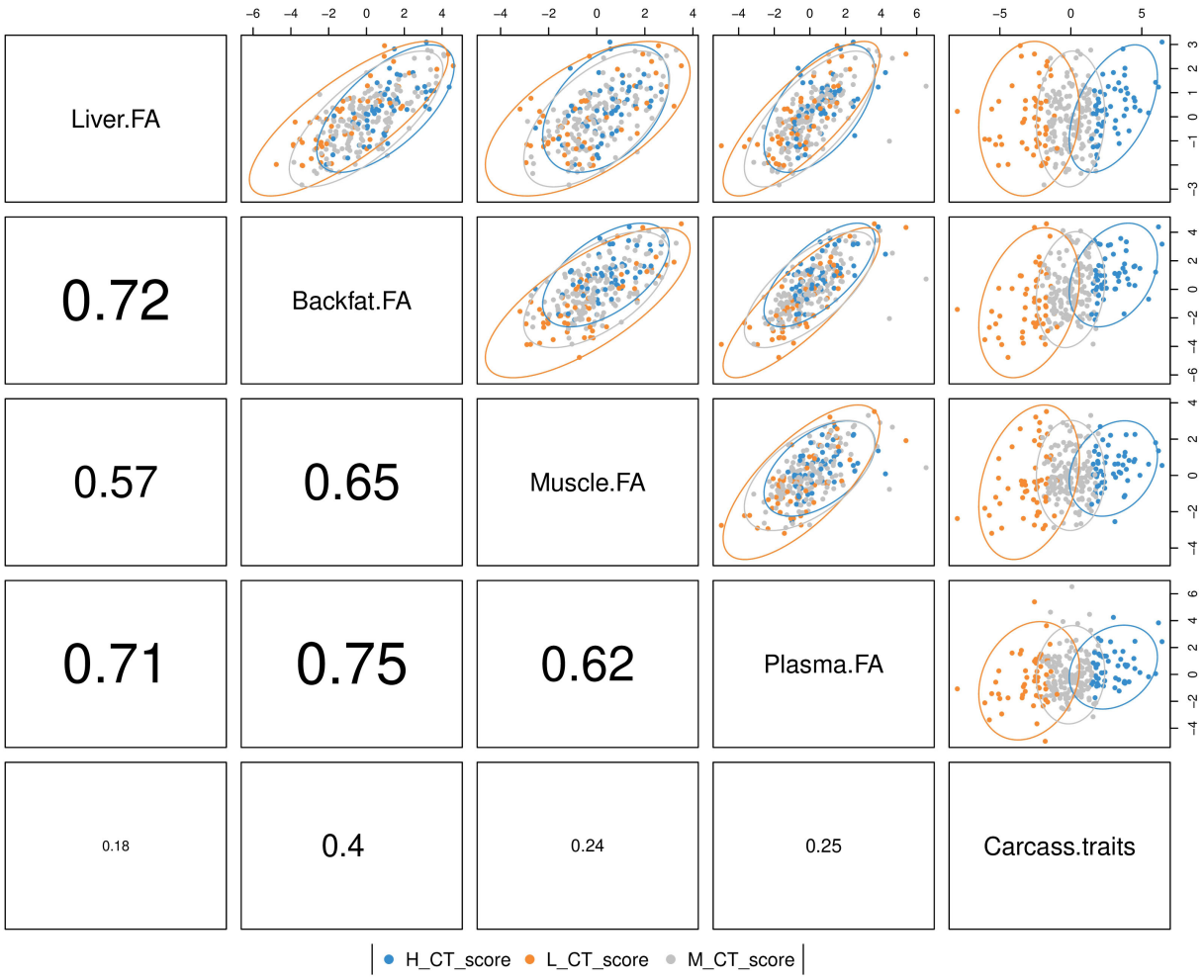

FIGURE 2
Correlation plots of fatty acids from different tissues with carcass traits. The individuals were grouped according to the carcass traits (CT) score, which were the first principal component score of carcass traits. H_CT_score, the group with high carcass traits score; L_CT_score, the group with low carcass traits score; M_CT_score, the group with medium carcass traits score.

3.3 Integrative analysis with carcass traits scores grouping

We identified the higher correlation between the PC1 of carcass traits and FAs from different tissues, especially the highest correlation (0.4) was for backfat FAs (Figure 2). The correlation between FAs in blood (0.25) and muscle (0.24) was lower, while the liver showed the weakest correlation (0.18) with carcass traits. The selected variables for the PC1 and their loading plots for each dataset can be found in Supplementary Figure 3. Five variables (FA traits) were selected for PC1 in liver and backfat, being C16:0 and C18:0 FAs the two variables with the highest contribution. In muscle, PC1 was characterized by five variables, with C20:2*n*-6 showing the highest contribution, followed by C16:0. For blood, seven variables were selected and C18:2*n*-6 had the highest impact for carcass traits, followed by C16:1*n*-7 and C18:1*n*-9. The distribution of individuals in PC1 and PC2 is displayed in Supplementary Figure 4, showing a discrimination of animals in two groups for backfat FAs and carcass traits. Figure 3 presents the distribution of the variables to the first two components. In muscle, an opposite distribution of C22:1*n*-9 and PUFA from C18:1*n*-9 and C16:0 was identified, as well as the opposite distribution of lean percentages and fat thickness. In addition, CW and fatness measures (BFT34 and HFT) clustered with blood C16:1*n*-7, C18:1*n*-7, C18:1*n*-9 and C18:2*n*-6 FA composition, as well as backfat C16:0, C18:0, C20:0, C18:1*n*-9, and C20:1*n*-9 FAs. The correlations among different datasets are depicted in Supplementary Figure 5, with a minimum correlation coefficient of 0.6. The network plot (Figure 4) used the same cutoff value (0.6). CW and fat thickness (BFT34 and HFT) were positively correlated with blood C16:1*n*-7, C18:1*n*-9, and C18:2*n*-6 FAs, liver C16:0, C18:0, and C18:1*n*-7 FAs, backfat C16:0, C18:0, C20:0, and C20:1*n*-9 FAs, and muscle C16:0 and C18:1*n*-9 FAs. Conversely, CW and fat thickness were negatively correlated with the PUFA composition in muscle. An opposite pattern is observed between the lean meat related traits (LM, LLM, HLM, SLM) with the FAs mentioned above in blood, liver, backfat, and muscle. Furthermore, loin thickness (LD34) was positively correlated with blood C14:0, liver C18:3*n*-3 and C20:5*n*-3, muscle C20:2*n*-6, and PUFA of backfat.

10.3389/fanim.2026.1763451

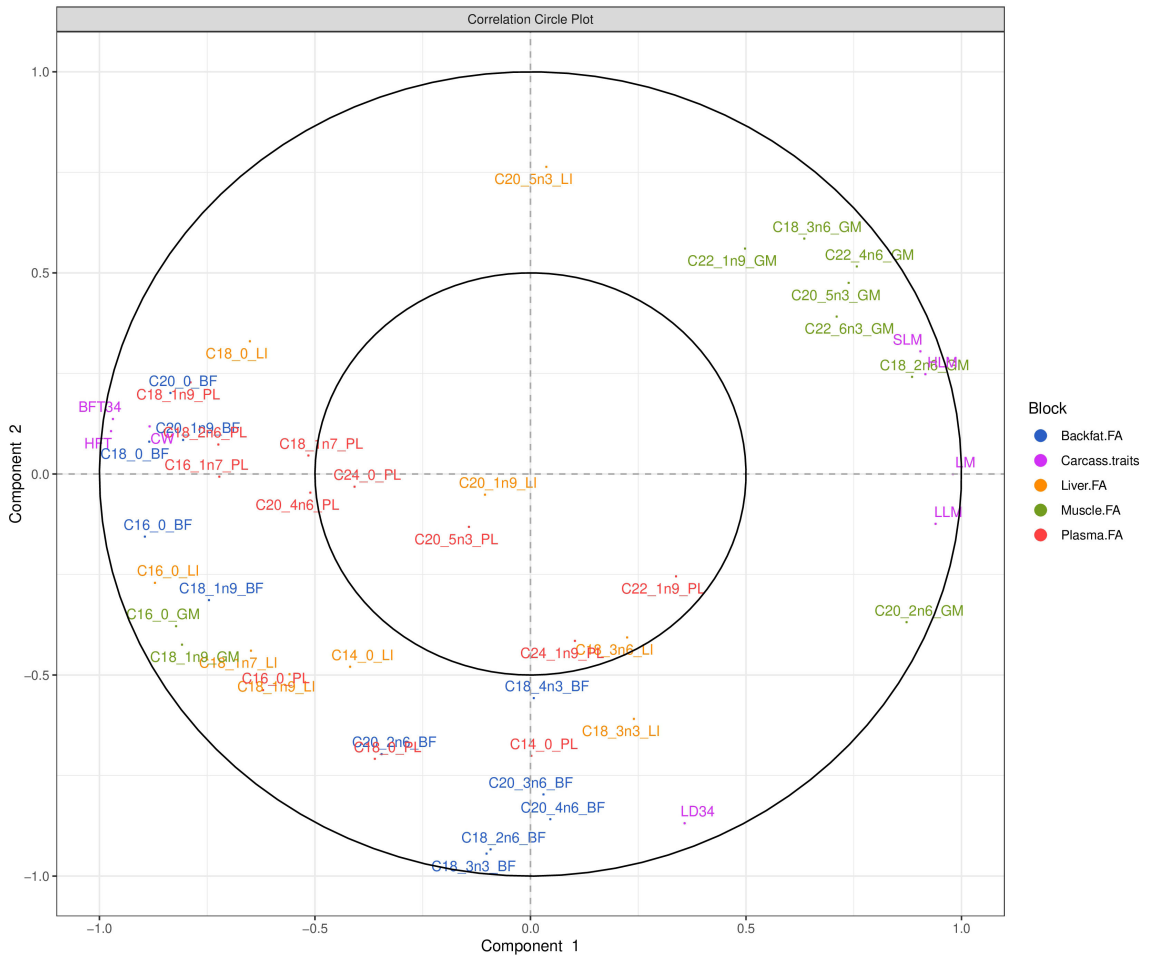

FIGURE 3
Correlation circle plot on the first and second components for the variables selected from different datasets. Backfat fatty acids are colored blue, carcass traits in purple, liver fatty acids in yellow, muscle fatty acids in green and plasma fatty acids in red. Each point represents a variable. The angle between variables reflects their pairwise correlations: acute angles indicate positive correlations, obtuse angles indicate negative correlations, and right angles indicate no correlation.

3.4 Integrative analysis with muscle fatty acid pattern score grouping

Within the muscle FA-pattern score grouping, the strongest correlation was observed between blood and backfat FA datasets (0.89), followed by backfat and muscle (0.85) and blood and muscle (0.82) (Figure 5). The distribution of animals into the first two components (Supplementary Figure 6) shows discrimination of individuals in groups for the FA composition of the four tissues. A correlation circle plot (Figure 6) illustrates the clustering of selected variables for PC1 and PC2. The selected variables for the PC1 and the loading plots of each dataset are in Supplementary Figure 7. According to PC1, a clear separation was observed between PUFA (C18:2*n*-6, C20:2*n*-6, C20:3*n*-6, C22:4*n*-6, and C20:5*n*-3) and MUFA (C16:0, C16:1*n*-7, and C18:1*n*-9) composition in both muscle and liver. The distribution of blood and backfat FAs was similar to what was observed in the grouping of carcass traits scores (Figure 3), with FAs such as C22:1*n*-9 and C24:1*n*-9 in blood closely associated with the PUFA in backfat. Additionally, C18:0 in backfat clustered with C18:1*n*-7, C18:1*n*-9, C18:2*n*-6, and C20:4*n*-6 FAs in blood. The correlation plot across different datasets displayed the PUFA of muscle almost completely negatively correlated the FAs in other tissues, with a cutoff 0.6 (Supplementary Figure 8). A network plot (Figure 7) was generated with Cytoscape for correlations higher than 0.6 among FAs. There were strong positive correlations (0.83 in average) of C16:0 across tissues. Additionally, the C16:0 in blood positively correlated with C18:1*n*-9 in backfat, muscle and liver, whereas it had a negative correlation with C18:2*n*-6 and C22:5*n*-3 in muscle. Additionally, the correlations of blood C18:0 with C16:0 in different tissues, C18:1*n*-9 in backfat and muscle, and muscle C18:2*n*-6 and C22:5*n*-3 were consistent with the correlations of blood C16:0 with these FAs. Moreover, the plasma C20:1*n*-9 and C22:1*n*-9 FAs were positively correlated with liver and backfat PUFA. A limited number of correlations between liver and backfat PUFA was observed: liver C20:4*n*-6 was negatively correlated (-0.67) with backfat C16:0 and liver C18:2*n*-6 was positively correlated (0.61) with backfat C20:4*n*-6. Moreover, we observed positive correlations among liver, backfat and muscle SFA (C14:0 and C16:0) and MUFA (C16:1*n*-7, C18:1*n*-7 and C18:1*n*-9). Conversely, the PUFA content in muscle exhibited a negative correlation with FAs from other tissues, regardless of whether they were SFAs, MUFAs, or PUFAs.

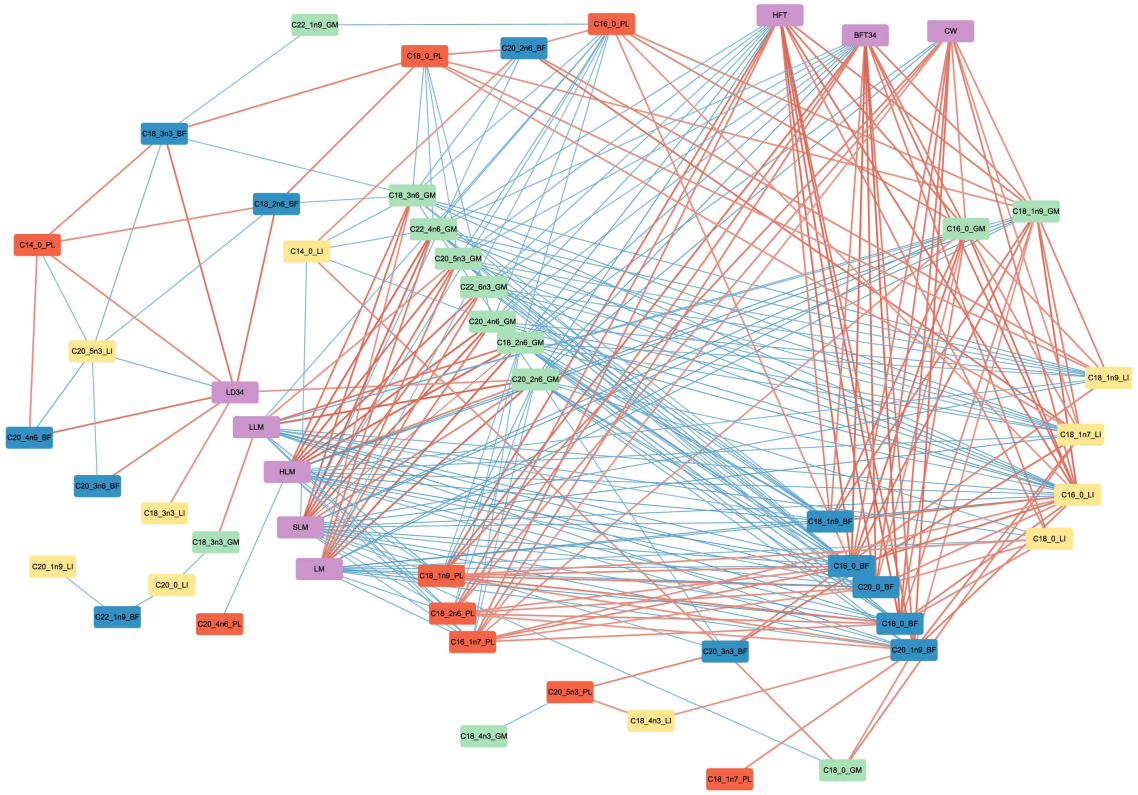

FIGURE 4
Relevance network with carcass traits score grouping represented in Cytoscape. Plot visualizing pairwise correlations (|r| > 0.6) among variables selected by the DIABLO model across the first 2 components. Features selected from blood fatty acids are indicated in red; in yellow, from liver; in blue, from backfat; in green, from muscle; and in purple, from carcass traits. Positive and negative correlations are indicated in red and blue lines, respectively. The intensity of connections reflects the strength of associations between variables from different tissues and phenotypic traits.

3.5 Prediction using 19 blood-derived fatty acids as predictors

To assess the full predictive potential of blood FA profiles, we initially performed prediction using all 19 available blood-derived FAs as input variables in the BayesC model. Figure 8A presents the correlations between predicted and observed values obtained using all 19 blood-derived FAs as predictors. The results show that muscle FA traits were predicted with high accuracy, with the highest median correlation observed for C16:0 in muscle (0.90). Note that muscle-derived C16:0 explains the largest variance across the muscle FAs in relation to PC1 as observed in Figure 1B. In contrast, the predictive ability for carcass traits was low to moderate, with median correlations ranging from 0.16 to 0.23.

3.6 Prediction using a subset of blood-derived fatty acids as predictors

To identify the most informative predictors, we calculated the posterior mean effect of each blood FA in each of the 15 training partitions (5-fold cross-validation repeated 3 times). For each predictor, we then computed the median of its posterior mean effects across the 15 folds. Figure 8B shows that the largest effects were detected for muscle FAs rather than carcass traits. These effects were primarily driven by a specific subset of blood FAs, including C16:0, C18:0, C18:1*n*-9, C18:2*n*-6, and C22:1*n*-9. Also, the signals of the predictors indicated an opposite effect between C16:0, C18:1*n*-9 and C18:2*n*-6 in muscle. This is in agreement with what we have already observed in the PCA figure (Figure 1B) of the muscle FAs where based on the first PC1 the C16:0 and C18:1*n*-9 have oppositive direction to C18:2*n*-6.

The four blood FAs with the highest median effects—C16:0, C18:0, C18:1*n*-9, and C18:2*n*-6—were selected as the reduced set of predictors for subsequent modeling. The choice of these four predictors was consistent with our observations from the DIABLO analysis (Supplementary Figure 7), where C16:0, C18:0, C18:1*n*-9, and C18:2*n*-6 derived from blood contributed most strongly to PC1.

Results in Figure 9 indicate that the prediction ability of the predictors on the muscle FAs is indeed mainly driven by the four selected blood FAs. The model using only blood-derived C16:0, C18:0, C18:1*n*-9, and C18:2*n*-6 captured between 94% and 98% of the predictive performance achieved by the model using the full set of predictors. This observation demonstrates comparable performance to the full model, indicating that these predictors capture the majority of the relevant signal. For carcass traits, the prediction ability of these four blood FAs was very similar to the full data set exhibiting again a low to moderate performance. Results mentioned above were implemented in BayesC with $\pi\_0 = 0.01$ which reflects a conservative prior belief that only a small fraction of predictors has non-zero effects, helping to mitigate potential overfitting and avoid overestimation of their effects. In

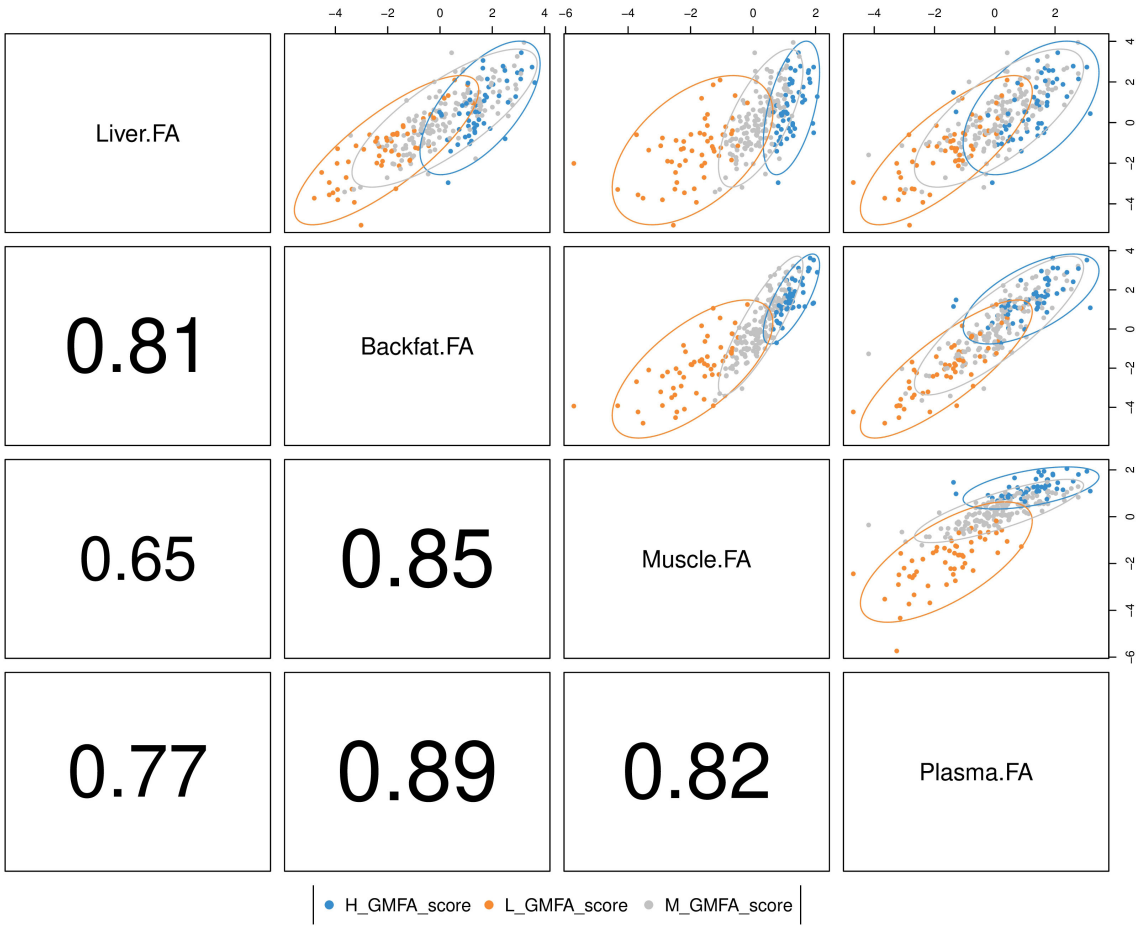

FIGURE 5
Correlation plots of fatty acids from different tissues. The individuals are grouped according to the muscle fatty acid pattern score (GMFA), which is the first principal component score of muscle fatty acid. H_GMFA_score, the group with high muscle fatty acid pattern score; L_GMFA_score, the group with low muscle fatty acid pattern score; M_GMFA_score, the group with medium muscle fatty acid pattern score.

contrast, $\pi\_0 = 0.25$ assumes a higher inclusion probability appropriate for targeted predictor set. Results were highly consistent across both priors in the full and reduced predictor analyses (Supplementary Figures 9, 10), supporting the robustness of our findings.

4 Discussion

Generally, pigs transition from the nursery to the growing phase at approximately 60 days of age (Wang et al., 2019), which represents a critical window of metabolic programming, during which lipid metabolism and adipose tissue development become increasingly active. Blood samples in our study were taken at the early stage of animal growth (around 60 days of age), whereas the samples of liver, backfat, and muscle were collected at slaughter (181 to 228 days). The study results revealed that blood MUFA (C16:1*n*-7 and C18:1*n*-9) and C18:2*n*-6, which had the highest contributions in predicting carcass traits, were positively correlated with CW and fat thickness (BFT34 and HFT) in slaughtered pigs, while being negatively correlated with lean meat related traits (LM, LLM, HLM, SLM), may be potential biomarkers for predicting carcass traits in slaughtered pigs in the current study. However, it is notable that the predication identified the most informative predictors is a specific subset of blood FAs, including C16:0, C18:0, C18:1*n*-9 and C18:2*n*-6, which exhibited the largest effects were detected for muscle FAs rather than carcass traits.

A human study identified that visceral fat area is positively correlated with the plasma levels of SFA, MUFA, and PUFA, which included the C18:2*n*-6 (Kang et al., 2017). The hyperlipolytic properties of the visceral adipose tissue can explain these results. Excess visceral fat releases large amounts of FAs, disturbing plasma FA metabolism by altering the composition of circulating FAs and changing the activities of FA desaturases (Kang et al., 2017). Rydén and Arner (2017) concluded that subcutaneous fat has a similar pattern to visceral fat and that lipolysis of subcutaneous fat influences circulating lipid levels. The subcutaneous adipose tissue represents the largest fat depot in the body, and the lipolysis of subcutaneous adipocytes is an important independent contributor to inter-individual variation in plasma lipids (Rydén and Arner, 2017). The alternations of lipid metabolism in adipose tissues are reflected in the free FAs in plasma, with adipose tissues being the major source of circulating free FAs (Cao et al., 2008). With increased FAs released and raised flux via the portal vein into the liver, there is an increase in FA availability in hepatocytes. This

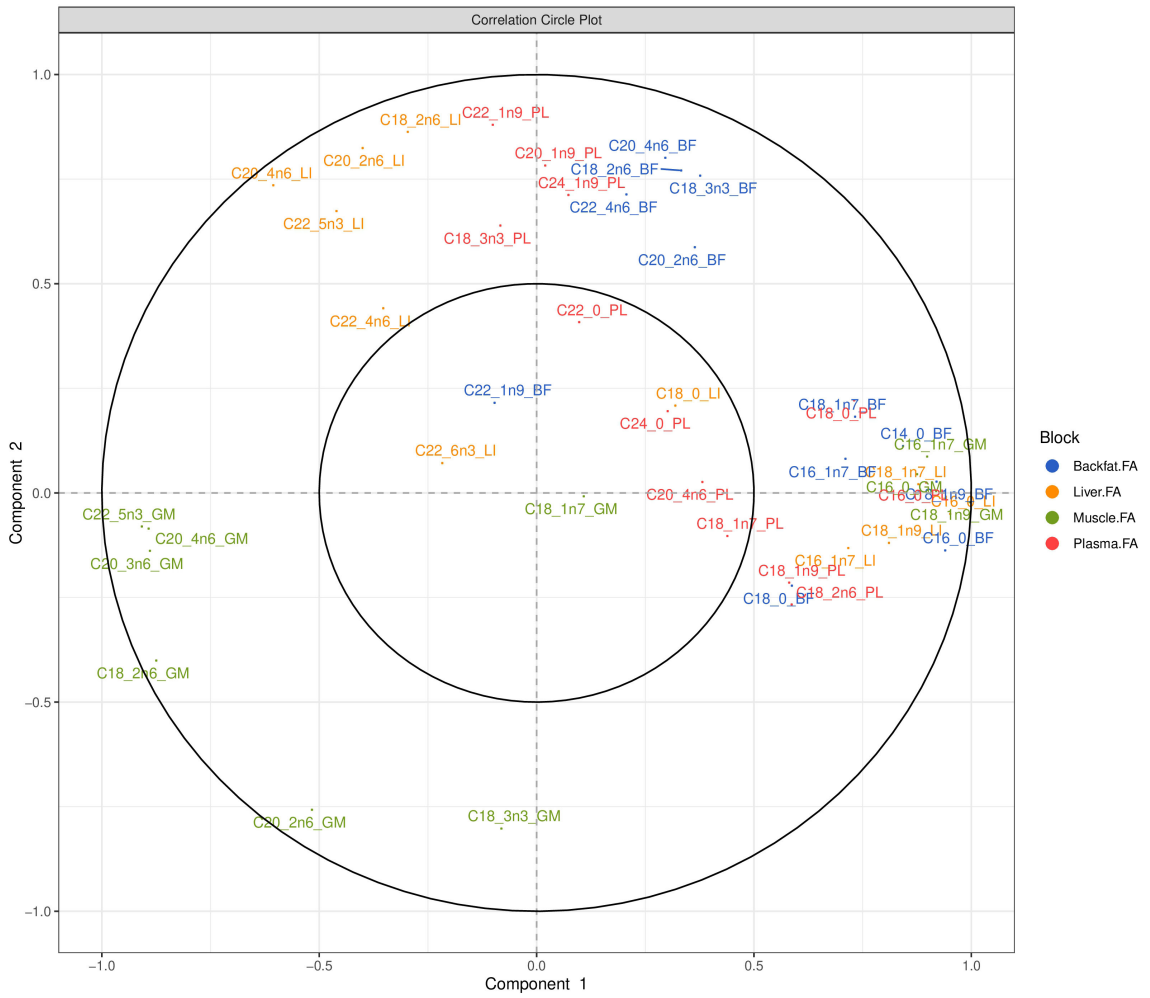

FIGURE 6
Correlation circle plot on the first and second components for the fatty acid variables selected from different tissues. Backfat fatty acids are colored blue, liver fatty acids in yellow, muscle fatty acids in green and plasma fatty acids in red. Each point represents a variable. The angle between variables reflects their pairwise correlations: acute angles indicate positive correlations, obtuse angles indicate negative correlations, and right angles indicate no correlation.

stimulates hepatic synthesis and secretion of TAG into the circulation via incorporation into lipoproteins, thereby increasing fat accumulation (Kang et al., 2017). Additionally, Kang et al. (2017) observed that individuals with larger visceral fat areas had higher levels of plasma C18:1*n*-9 and C16:1*n*-7, along with enhanced activity of 16:1*n*-7/16:0 desaturase (C16-SCD). They concluded that individuals with higher levels of C16:1*n*-7 and increased C16-SCD activity are more likely to exacerbate fat accumulation.

C18:2*n*-6 is provided from the diet as one of the essential FAs, and its content is affected by the composition of the diet. Grains and vegetable oils such as sunflower, corn, and soybean are the basements of feeding in pig production systems and enrich N6 PUFA, especially the C18:2*n*-6 (Almeida et al., 2021). Guillevic et al. (2009) reported that feeding the sunflower diet significantly lowers the subcutaneous adipose tissue weight in pigs. Additionally, Gol et al. (2019) evaluated the genetic relationships of C18:2*n*-6 of IMF as a biomarker of lean growth traits in the Duroc line by identifying the genetic correlation pattern of C18:2*n*-6 (absolute value) with IMF is 0.88. However, the content of C18:2*n*-6 of blood exhibits the opposite correlation with fat deposition trait, and the prediction ability of C18:2*n*-6 exhibited a low to moderate performance for carcass traits. An explanation for this is the effect of N6 PUFA depends on the intracellular level of cAMP (Madsen et al., 2008). Elevated cAMP can activate protein kinase, further inducing the expression and activity of cyclooxygenase, thereby allowing N6 PUFA to exert an anti-adipogenic role. Different diets can lead to variations in cAMP levels. Mice fed a protein-rich diet experience an increase in the glucagon/insulin ratio, which subsequently promotes cAMP-dependent signaling and induces cyclooxygenase-mediated prostaglandin synthesis, ultimately reducing adipose tissue mass (Madsen et al., 2008). In fact, the majority of the studies did not observe a clear correlation between N6 PUFA supplement and carcass performance (Minelli et al., 2023; Realini et al., 2010; Song et al., 2020). Some studies suggest that N6 PUFA promotes adipose tissue development (Madsen et al., 2008; Massiera et al., 2010), while diets rich in conjugated linoleic acid reduce adipose mass (Norris et al., 2009).

Additionally, the current study observed that the crosstalk of FAs in liver, muscle and backfat consistently displays that C16:0, C18:0, and C18:1*n*-9 were positively correlated with both CW and

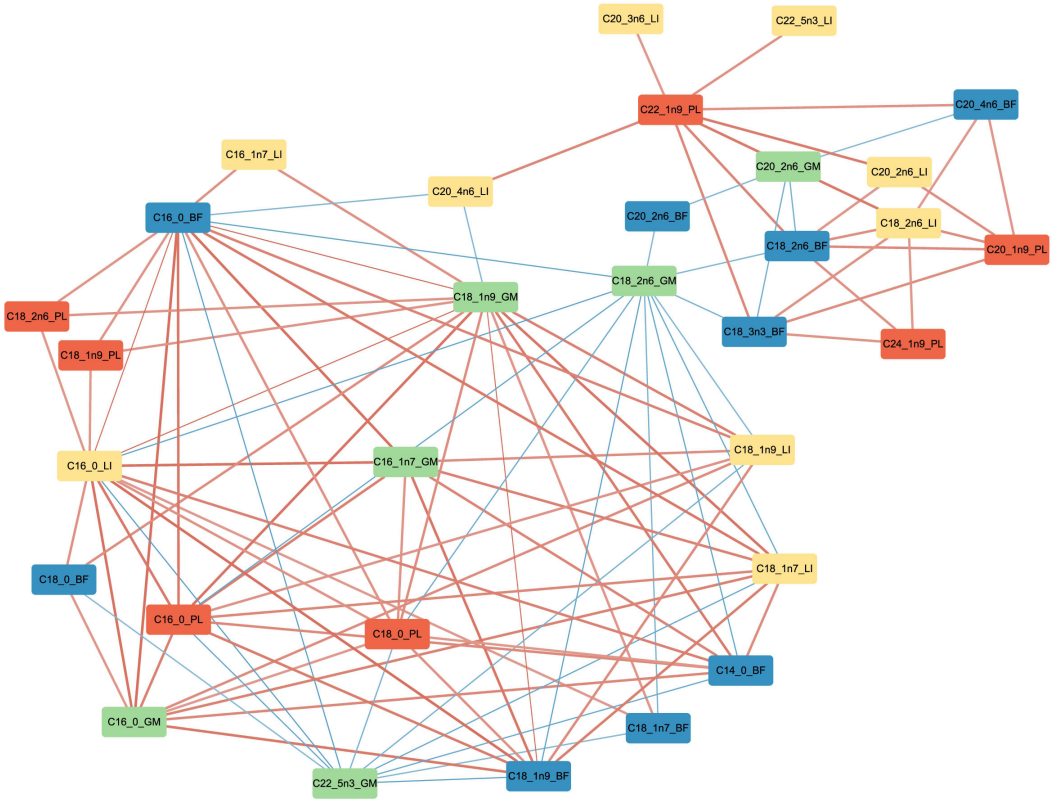

FIGURE 7
Relevance network with muscle fatty acid score grouping represented in Cytoscape. Plot visualizing pairwise correlations (|r| > 0.6) among variables selected by the DIABLO model across the first 2 components. Features selected from blood fatty acids are indicated in red; in yellow, from liver; in blue, from backfat; in green, from muscle. Positive and negative correlations are indicated in red and blue nodes, respectively. The intensity of connections reflects the strength of associations between variables from different tissues.

fat thickness, while being negatively correlated with lean percentage in meats (HLM, SLM, LM and LLM). Conversely, PUFA in muscle exhibits the opposite association. Since the FA composition of muscle is a crucial factor in meat quality and, consequently, influences customer preferences, we explored the correlation of muscle FA profiles with those of other tissues to identify biomarkers in the blood of young animals for meat quality. In our study, we found that the presence of C16:0 and C18:0 in blood exhibited positive correlations with C16:1*n*-7, C18:1*n*-7 and C18:1*n*-9 levels observed in liver, backfat, and muscle, while demonstrating an inverse relationship with PUFA content within muscle. Furthermore, these by using intracellular acetyl-CoA as a substrate, resulting in the production of C16:0, which can be further elongated to C18:0 and C20:0. Both C16:0 and C18:0 can be desaturated to form 16:1*n*-9 and 18:1*n*-9, respectively. The results of the prediction also confirmed that the C16:0, C18:0 and C18:1*n*-9 in the blood have a great ability to predict the contents of C16:0, C18:1n-9, and PUFA C18:2*n*-6.

The aliphatic tails of long-chain FAs exceeding 12 carbons are slowly absorbed and metabolized in the organism, resulting in rapid accumulation in both liver and adipose tissue (Sarmiento-García and Vieira-Aller, 2023). Plasma lipid concentrations influence the rate of uptake of free FAs into muscle, in which FAs are utilized as fuel by being absorbed as free FAs and converted into long-chain fatty acyl-CoAs and imported into mitochondria via carnitine acyltransferases for beta-oxidation (Corcoran et al., 2007). In addition to the physiological metabolism of FAs across tissues, the C16:0 and C18:0 are the main products of the *de novo* FA synthesis pathway and are further converted to MUFA (C16:1*n*-7 and C18:1*n*-9) by the SCD within the same tissue. The highest expression of *SCD* has been reported in liver and adipose tissue (Doran et al., 2006). In particular, the desaturase index C16-SCD showed high correlations across tissues, and the 16:1*n*-7/16:0 ratio in free FA effectively reflects the activity of SCD in adipose tissue (Warensjö et al., 2009). Additionally, as stated before, the 16:1*n*-7/16:0 index was positively associated with human obesity (Warensjö et al., 2006). In animal organisms, fat accumulation is produced through adipogenesis and lipogenesis, and in pigs these processes occur mainly in the adipose tissue (Nguyen et al., 2021). The primary role of FAs in adipose tissue involves their storage as TAG within mature adipocytes, contributing to the consequences of excessive accumulation observed in obesity. In general, pigs with higher fat deposition tend to have higher percentages of SFA and MUFA, as well as a lower content of PUFA in adipose tissue and muscle (Yang et al., 2010). Our study is in accordance with these observations: the SFA (C16:0, C18:0 and C20:0) and MUFA (C18:1*n*-9 and C20:1*n*-9) in both adipose tissue and muscle, were positively correlated with fat thickness (BFT34 and HFT), and negatively correlated with lean meat percentages. However, PUFA exhibited opposite correlations with fat thickness and lean meat

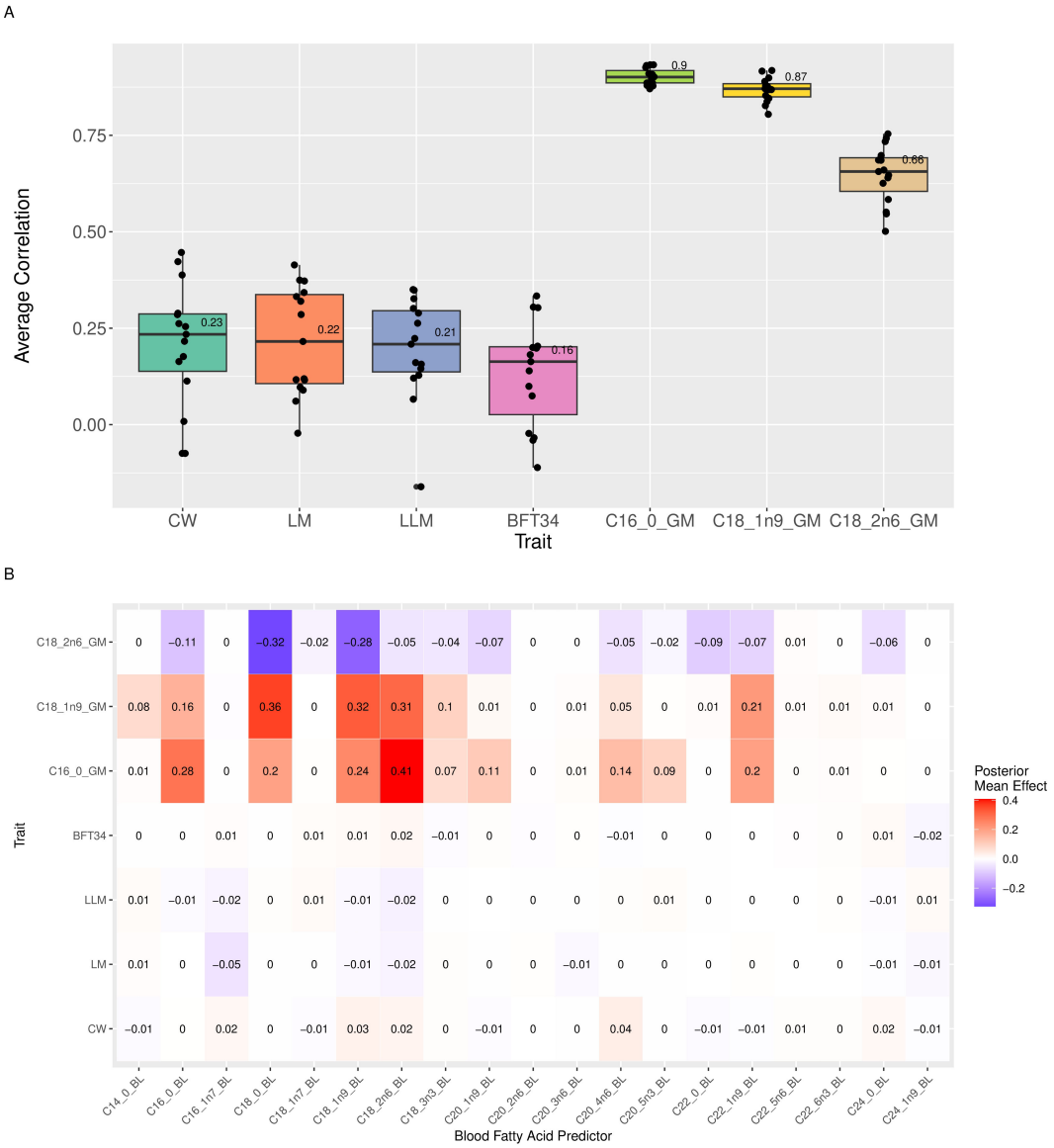

FIGURE 8
(A) Boxplot of the correlation values across the 5-fold x 3 cross validation strategy and the corresponding median value for each trait using the full set of blood-derived fatty acids as predictors; **(B)** heatmap of the median value of predictor´s posterior mean effect across partitions for the 19 blood-derived blood fatty acids.

percentages. As pigs approach market weight, the influence of dietary factors on the FA profile diminishes, and the impact of *de novo* FA synthesis increases (Harsh and Boler, 2024). Kloareg et al. (2007) also demonstrated this point, showing that the deposition of dietary FAs into tissues is relatively minor compared to endogenous FAs synthesis and the composition of *de novo* synthesized FA. As the fattening period increases, Ayuso et al. (2020) observed an increase in MUFA in backfat, primarily due to the higher level of C18:1*n*-9, and a decrease in PUFA in both backfat and IMF, while there were no notable changes in SFA content.

On the other hand, the observation in our study that the PUFA content in adipose tissue and muscle was negatively correlated with fat thickness may be explained by the decrease of the size of adipocytes. The adipocyte, as the only cell that can significantly change in size under physiological conditions, has the metabolic capacity to accumulate and mobilize TAG, thereby influencing adipose tissue development (Garaulet et al., 2006). A study in humans revealed that the size of adipocytes is inversely correlated with the PUFA content in subcutaneous adipose tissue, likely due to higher desaturase activity and consequent higher *de novo* lipogenesis (Garaulet et al., 2006). Sessler et al. also addressed that PUFA down-regulates fat synthesis and accumulation in mature adipocytes (Sessler and Ntambi, 1998). The N3 PUFA has been reported to inhibit the FA synthesis, increasing FA oxidation and reducing TAG synthesis as natural ligands for PPAR suppress the transcription of lipogenic genes (Duan et al., 2014; Surette et al., 1992; Willumsen et al., 1993). For instance, C20:5*n*-3 and C22:6*n*-3 are closely associated with the expression of genes encoding lipogenic enzymes (fatty acid synthetase, LPL), lipolysis (hormone-sensitive lipase), transcription factors (C/EBPa), and leptin, whose changes in mRNA level led to a decrease in the size of adipocytes (Garaulet et al., 2006; Raclot et al., 1997).

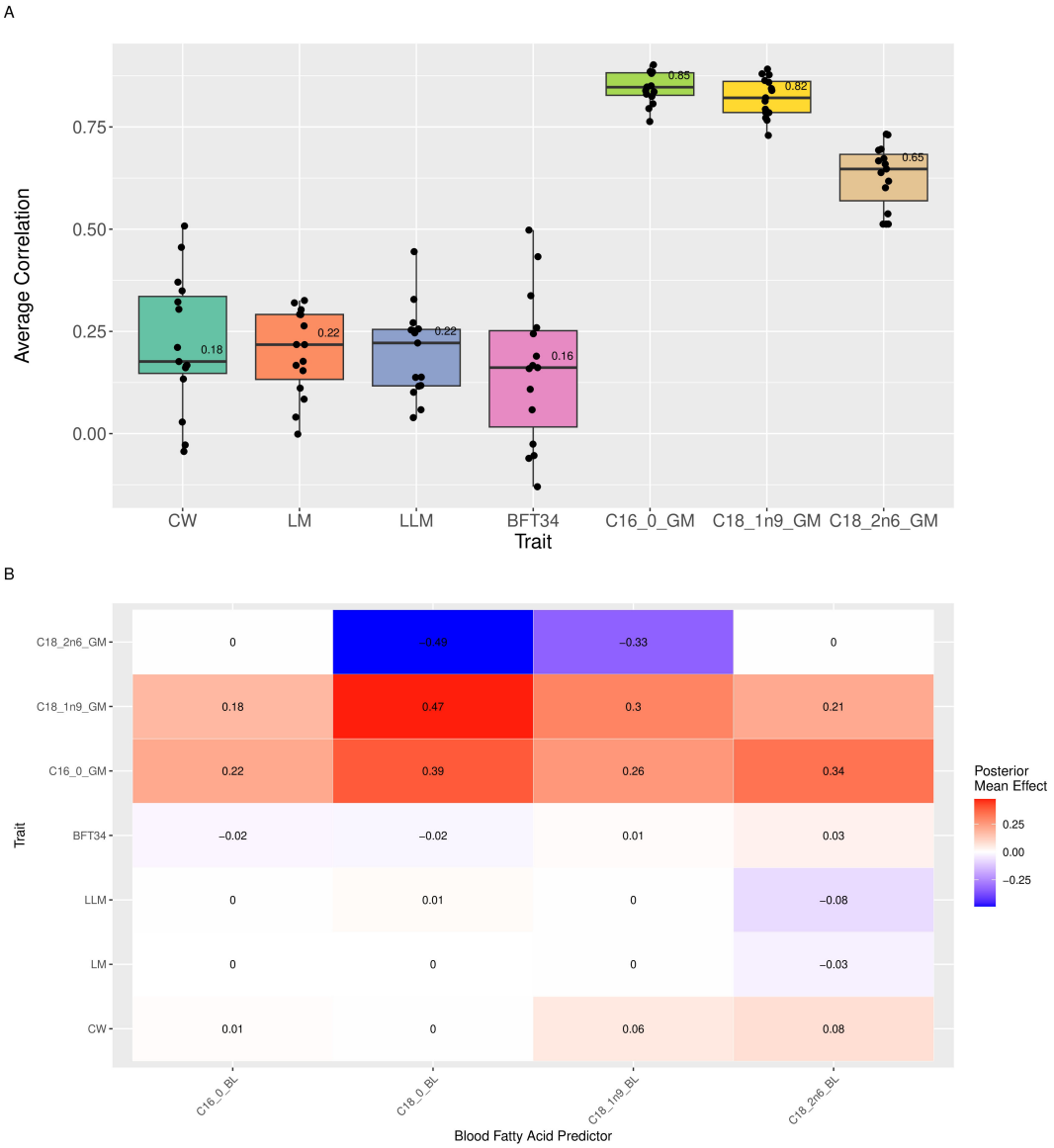

FIGURE 9
(A) Boxplot of the correlation values across the 5-fold x 3 cross validation strategy and the corresponding median value for each trait using the four selected blood-derived fatty acids as predictors; **(B)** heatmap of the median value of predictor´s posterior mean effect across partitions for the blood-derived C16:0, C18:0, C18:1n-9, and C18:2n-6.

Additionally, our previous studies observed that miR-33a and miR-33b negatively correlated with PUFA content and co-transcribed with SREBF1 and SREBF2, which involve FA and cholesterol metabolism (Criado-Mesas et al., 2021).

It is interesting to note that the C16:1*n*-7 as the desaturase product of biomarker C16:0 identified in the current study, is an adipokine released by adipose tissues and participates in diverse metabolic processes (Bermúdez et al., 2022). In addition to C16:1*n*-7 regulates FA synthesis and activates lipogenesis, regulates inflammation and oxidative stress in muscle (Gu et al., 2023). Cao et al. (2008) reported that in fatty acid–binding proteins (FABP) 4 and 5 deficiency mice, the C16:1*n*-7 is the major lipid regulating the expression of *SCD* and stimulate muscle glucose uptake and TAG accumulation to improve glucose homeostasis and insulin sensitivity. Additionally, the C16:1*n*-7 plays a role in reducing inflammation in metabolically active tissues (Frigolet and Gutiérrez-Aguilar, 2017). In mice macrophage, the C16:1*n*-7 treatment reduced the expression of pro-inflammatory genes and secretion of cytokine by AMP-activated protein kinase exert anti-inflammatory, whereas the C16:0 had the opposite effect (Chan et al., 2015). It is widely accepted that C16:1*n*-7 as biomarker in human health and plays crucial roles in both physiology and pathophysiology, whereas it has rarely been proposed as a biomarker in robustness in domestic animals. Additionally, numerous studies have shown that the FAs regulate the function of immune cells regardless of the categories of FAs. Kratz et al. (2014) discovered that the macrophage of adipose tissues treated by SFA palmitate triggers metabolic activation. The palmitate plays the proinflammatory role by binding to the Toll-like receptor on the cell surface and releasing cytokine, while the internalization of palmitate activates P62 and PPARγ, consequently promoting lipid metabolism and anti-inflammatory. Moreover, the activations and

differentiation of T and B cells are associated with FA metabolism (Zhou et al., 2023). During the differentiation of $CD4^+$ T cells to T helper 17 cells, where the energy metabolism alters from relying on glucose as an energy source to increasing FA synthesis (Berod et al., 2014). In addition, activated B cells showed higher levels of SCD activity and MUFA, which promote the proliferation of B cells and maintain their health (Zhou et al., 2021).

Therefore, the FAs crosstalk involves both growth and immunocompetence in organisms. However, FA deposition in various tissues is influenced by the dynamic supply of FAs, where FA capture is affected by the development rate of the tissues (Kloareg et al., 2007). Consequently, FA deposition changes throughout the growth process, and FAs are preferentially deposited in some tissues. Increasing the sampling time point in further studies is important to elucidate the mechanism of FA dynamic deposition in different tissues. Additionally, from a practical breeding perspective, the associations identified between plasma FAs and carcass traits provide the possibility of using blood metabolites as indirect selection tools in breeding programs. Carcass traits are typically measured postmortem, limiting selection accuracy and increasing generation intervals. Therefore, if the observed correlation reflects an underlying genetic relation, plasma FAs measurable in live animals could facilitate early-life selection. The genetic parameters for these traits have already been published by Hernández-Banqué et al. (2025), further research should focus on validating predictive potential in the population.

5 Conclusions

In summary, plasma levels of C16:0 and C16:1*n*-7, along with their ratio and accompanying with C18:1*n*-9 and C18:2*n*-6, emerge as major candidate indicators for predicting their content in the liver, backfat, and muscle of slaughtered pigs, as well as for predicting carcass traits. Additionally, tissue-cross talk was observed, with C16:0 and C18:0 in blood positively correlated with C16:1*n*-7, C18:1*n*-7 and C18:1*n*-9 levels in the liver, backfat, and muscle. However, they exhibited an opposite relationship with PUFA content of muscle in our study.

Data availability statement

The original contributions presented in the study are included in the article/Supplementary Material. Further inquiries can be directed to the corresponding authors.

Ethics statement

The animal study was approved by Institute of Agricultural Research and Technology (IRTA). The study was conducted in accordance with the local legislation and institutional requirements.

Author contributions

JL: Data curation, Formal analysis, Visualization, Writing – original draft. I-TV: Data curation, Formal analysis, Validation, Writing – review & editing. CS: Formal analysis, Methodology, Writing – review & editing. FL: Investigation, Software, Writing – review & editing. AS: Funding acquisition, Supervision, Writing – review & editing. AC: Investigation, Writing – review & editing. YR: Data curation, Formal analysis, Writing – review & editing. MB: Conceptualization, Funding acquisition, Supervision, Writing – review & editing. JF: Conceptualization, Data curation, Funding acquisition, Supervision, Writing – review & editing.

Funding

The author(s) declared that financial support was received for this work and/or its publication. This research was financially supported as part of the projects METAPIGEN PID2020-112677RB-C21-22 and METAPIGSEL PID2023-148961OB-C21-22 funded by MCIN/ AEI /10.13039/501100011033 and by "ERDF A way of making Europe". We also acknowledge the support from H2020 GENE-SWitCH (grant agreement n° 817998) project, CEX2019-000902-S funded by MCIN/AEI/10.13039/501100011033, and the CERCA Programme, Generalitat de Catalunya. In addition, J. Liu was funded by a Ph.D. fellowship from the China Scholarship Council (CSC), C. Sebastià was funded with a FI-AGAUR PhD grant from the Generalitat de Catalunya (2020FI_B_00225), F. Llobet-Cabau was funded with a Joan Oró FI-AGAUR Ph.D. grant from the Generalitat de Catalunya (2023 FI-1 00171).

Acknowledgments

We appreciate the cooperation of the technicians of IRTA and Selección Batallé S.A during the experimental process on the farm and in the slaughterhouse. IRBLleida Lipidomics Core Facility – PLICAT and the NUTRICAL-UCM laboratory supported the identification and quantification of FA.

Conflict of interest

The author(s) declared that this work was conducted in the absence of any commercial or financial relationships that could be construed as a potential conflict of interest.

The author YR declared that they were an editorial board member of Frontiers, at the time of submission. This had no impact on the peer review process and the final decision.

Generative AI statement

The author(s) declared that generative AI was not used in the creation of this manuscript.

Any alternative text (alt text) provided alongside figures in this article has been generated by Frontiers with the support of artificial intelligence and reasonable efforts have been made to ensure accuracy, including review by the authors wherever possible. If you identify any issues, please contact us.

Publisher's note

All claims expressed in this article are solely those of the authors and do not necessarily represent those of their affiliated organizations, or those of the publisher, the editors and the reviewers. Any product that may be evaluated in this article, or claim that may be made by its manufacturer, is not guaranteed or endorsed by the publisher.

Supplementary material

The Supplementary Material for this article can be found online at: https://www.frontiersin.org/articles/10.3389/fanim.2026.1763451/full#supplementary-material

References

Almeida, V. V., Silva, J. P. M., Schinckel, A. P., Meira, A. N., Moreira, G. C. M., Gomes, J. D., et al. (2021). Effects of increasing dietary oil inclusion from different sources on growth performance, carcass and meat quality traits, and fatty acid profile in genetically lean immunocastrated male pigs. *Livest. Sci.* 248, 104515. doi: 10.1016/j.livsci.2021.104515

Anderson, S. G., Sanders, T. A. B., and Cruickshank, J. K. (2009). Plasma fatty acid composition as a predictor of arterial stiffness and mortality. *Hypertension* 53, 839–845. doi: 10.1161/HYPERTENSIONAHA.108.123885

Ayuso, D., González, A., Peña, F., Hernández-García, F. I., and Izquierdo, M. (2020). Effect of fattening period length on intramuscular and subcutaneous fatty acid profiles in Iberian pigs finished in the Montanera sustainable system. *Sustain. (Switzerl).* 12, 7937. doi: 10.3390/SU12197937

Bajerska, J., Skoczek-Rubińska, A., Małczak, L., Vucic, V., Arsic, A., Kojadinovic, M., et al. (2023). Plasma fatty acid composition and some markers of dietary habits are associated with cardiovascular disease risk determined by an atherogenic plasma index in postmenopausal women. *Nutr. Res.* 115, 47–60. doi: 10.1016/j.nutres.2023.05.008

Bermúdez, M. A., Pereira, L., Fraile, C., Valerio, L., Balboa, M. A., and Balsinde, J. (2022). Roles of palmitoleic acid and its positional isomers, hypogeic and sapienic acids, in inflammation, metabolic diseases and cancer. *Cells* 11, 2146. doi: 10.3390/cells11142146

Berod, L., Friedrich, C., Nandan, A., Freitag, J., Hagemann, S., Harmrolfs, K., et al. (2014). *De novo* fatty acid synthesis controls the fate between regulatory T and T helper 17 cells. *Nat. Med.* 20, 1327–1333. doi: 10.1038/nm.3704

Cao, H., Gerhold, K., Mayers, J. R., Wiest, M. M., Watkins, S. M., and Hotamisligil, G. S. (2008). Identification of a lipokine, a lipid hormone linking adipose tissue to systemic metabolism. *Cell* 134, 933–44. doi: 10.1016/j.cell.2008.07.048

Chan, K. L., Pillon, N. J., Sivaloganathan, D. M., Costford, S. R., Liu, Z., Théret, M., et al. (2015). Palmitoleate reverses high fat-induced proinflammatory macrophage polarization via AMP-activated protein kinase (AMPK). *J. Biol. Chem.* 290, 16979–16988. doi: 10.1074/jbc.M115.646992

Corcoran, M. P., Lamon-Fava, S., and Fielding, R. A. (2007). Skeletal muscle lipid deposition and insulin resistance: effect of dietary fatty acids and exercise. *Am. J. Clin. Nutr.* 83, 662–677. doi: 10.1093/ajcn/85.3.662

Criado-Mesas, L., Ballester, M., Crespo-Piazuelo, D., Passols, M., Castelló, A., Sánchez, A., et al. (2021). Expression analysis of porcine miR-33a/b in liver, adipose tissue and muscle and its potential role in fatty acid metabolism. *PloS One* 16, e0245858. doi: 10.1371/journal.pone.0245858

Dooley, C., and Ryan, A. S. (2019). Role of dietary macronutrients and fatty acids in obesity and metabolic risk in older adults. *Int. J. Obes. Nutr. Sci.* 1, 6–10. doi: 10.18689/ijons-1000102

Doran, O., Moule, S. K., Teye, G. A., Whittington, F. M., Hallett, K. G., and Wood, J. D. (2006). A reduced protein diet induces stearoyl-CoA desaturase protein expression in pig muscle but not in subcutaneous adipose tissue: relationship with intramuscular lipid formation. *Br. J. Nutr.* 95, 609–617. doi: 10.1079/bjn20051526

Duan, Y., Li, F., Li, L., Fan, J., Sun, X., and Yin, Y. (2014). n-6:n-3 PUFA ratio is involved in regulating lipid metabolism and inflammation in pigs. *Br. J. Nutr.* 111, 445–451. doi: 10.1017/S0007114513002584

Fernandez, C., Sandin, M., Sampaio, J. L., Almgren, P., Narkiewicz, K., Hoffmann, M., et al. (2013). Plasma lipid composition and risk of developing cardiovascular disease. *PloS One* 8, e71846. doi: 10.1371/journal.pone.0071846

Frayn, K. N., Arner, P., and Yki-Järvinen, H. (2006). Fatty acid metabolism in adipose tissue, muscle and liver in health and disease. *Essays. Biochem.* 42, 89–103. doi: 10.1042/bse0420089

Frigolet, M. E., and Gutiérrez-Aguilar, R. (2017). The role of the novel lipokine palmitoleic acid in health and disease. *Adv. Nutr.* 8, 173S–181S. doi: 10.3945/an.115.011130

Garaulet, M., Hernandez-Morante, J. J., Lujan, J., Tebar, F. J., and Zamora, S. (2006). Relationship between fat cell size and number and fatty acid composition in adipose tissue from different fat depots in overweight/obese humans. *Int. J. Obes. (Lond).* 30, 899–905. doi: 10.1038/sj.ijo.0803219

Gligorijević, V., and Pržulj, N. (2015). Methods for biological data integration: perspectives and challenges. *J. R. Soc. Interface* 12, 20150571. doi: 10.1098/rsif.2015.0571

Gol, S., González-Prendes, R., Bosch, L., Tor, M., Reixach, J., Pena, R. N., et al. (2019). Linoleic acid metabolic pathway allows for an efficient increase of intramuscular fat content in pigs. *J. Anim. Sci. Biotechnol.* 10, 33. doi: 10.1186/s40104-019-0343-8

Gu, X., Wang, L., Liu, S., and Shan, T. (2023). Adipose tissue adipokines and lipokines: Functions and regulatory mechanism in skeletal muscle development and homeostasis. *Metabolism* 139, 155379. doi: 10.1016/j.metabol.2022.155379

Guillevic, M., Kouba, M., and Mourot, J. (2009). Effect of a linseed diet or a sunflower diet on performances, fatty acid composition, lipogenic enzyme activities and stearoyl-CoA-desaturase activity in the pig. *Livest. Sci.* 124, 288–294. doi: 10.1016/j.livsci.2009.02.009

Harsh, B., and Boler, D. (2024). "Swine breeds versus genetic lines," in *Encyclopedia of Meat Sciences*. Ed. M. Dikeman (Amsterdam: Academic Press), 488–494.

Hernández-Banqué, C., Liu, J., Jové-Juncà, T., González-Rodríguez, O., Portero-Otín, M., Folch, J. M., et al. (2025). Genetic determinism of fatty acid composition in liver, muscle, backfat and plasma and its link to immunocompetence and performance in pigs. *Sci. Rep.* 15, 43982. doi: 10.1038/s41598-025-27713-3

Hodson, L., McQuaid, S. E., Karpe, F., Frayn, K. N., and Fielding, B. A. (2008). Differences in partitioning of meal fatty acids into blood lipid fractions: a comparison of linoleate, oleate, and palmitate. *Am J Physiol Endocrinol Metab.* 296, E64–71. doi: 10.1152/ajpendo.90730.2008

Jové, M., Cabré, R., Mota-Martorell, N., Martin-Garí, M., Obis, È., Ramos, P., et al. (2021). Age-related changes in lipidome of rat frontal cortex and cerebellum are partially reversed by methionine restriction applied in old age. *Int. J. Mol. Sci.* 22, 12517. doi: 10.3390/ijms222212517

Jové-Juncà, T., Crespo-Piazuelo, D., González-Rodríguez, O., Pascual, M., Hernández-Banqué, C., Reixach, J., et al. (2024). Genomic architecture of carcass and pork traits and their association with immune capacity. *Animal* 18, 101043. doi: 10.1016/j.animal.2023.101043

Kang, M., Lee, A., Yoo, H. J., Kim, M., Kim, M., Shin, D. Y., et al. (2017). Association between increased visceral fat area and alterations in plasma fatty acid profile in overweight subjects: a cross-sectional study. *Lipids Health Dis.* 16, 248. doi: 10.1186/s12944-017-0642-z

Kloareg, M., Noblet, J., and Van Milgen, J. (2007). Deposition of dietary fatty acids, *de novo* synthesis and anatomical partitioning of fatty acids in finishing pigs. *Br. J. Nutr.* 97, 35–44. doi: 10.1017/S0007114507205793

Kratz, M., Coats, B. R., Hisert, K. B., Hagman, D., Mutskov, V., Peris, E., et al. (2014). Metabolic dysfunction drives a mechanistically distinct proinflammatory phenotype in adipose tissue macrophages. *Cell Metab.* 20, 614–625. doi: 10.1016/j.cmet.2014.08.010

Lim, S. A., Su, W., Chapman, N. M., and Chi, H. (2022). Lipid metabolism in T cell signaling and function. *Nat. Chem. Biol.* 18, 470–481. doi: 10.1038/s41589-022-01017-3

Liu, Q., Matthan, N. R., Manson, J. E., Howard, B. V., Tinker, L. F., Neuhouser, M. L., et al. (2019). Plasma phospholipid fatty acids and coronary heart disease risk: A

matched case-control study within the women's health initiative observational study. *Nutrients* 11, 1672. doi: 10.3390/nu11071672

Madsen, L., Pedersen, L. M., Liaset, B., Ma, T., Petersen, R. K., Van Den Berg, S., et al. (2008). cAMP-dependent signaling regulates the adipogenic effect of n-6 polyunsaturated fatty acids. *J. Biol. Chem.* 283, 7196–7205. doi: 10.1074/jbc.M707775200

Malgwi, I. H., Halas, V., Grünvald, P., Schiavon, S., and Jócsák, I. (2022). Genes related to fat metabolism in pigs and intramuscular fat content of pork: A focus on nutrigenetics and nutrigenomics. *Anim. (Basel).* 12, 150. doi: 10.3390/ani12020150

Massiera, F., Barbry, P., Guesnet, P., Joly, A., Luquet, S., Moreilhon-Brest, C., et al. (2010). A Western-like fat diet is sufficient to induce a gradual enhancement in fat mass over generations. *J. Lipid Res.* 51, 2352–2361. doi: 10.1194/jlr.M006866

Minelli, G., D'Ambra, K., Macchioni, P., and Lo Fiego, D. P. (2023). Effects of pig dietary n-6/n-3 polyunsaturated fatty acids ratio and gender on carcass traits, fatty acid profiles, nutritional indices of lipid depots and oxidative stability of meat in medium–heavy pigs. *Foods* 12, 4106. doi: 10.3390/foods12224106

Nguyen, D. V., Nguyen, O. C., and Malau-Aduli, A. E. O. (2021). Main regulatory factors of marbling level in beef cattle. *Vet. Anim. Sci.* 14, 100219. doi: 10.1016/j.vas.2021.100219

Norris, L. E., Collene, A. L., Asp, M. L., Hsu, J. C., Liu, L.-F., Richardson, J. R., et al. (2009). Comparison of dietary conjugated linoleic acid with safflower oil on body composition in obese postmenopausal women with type 2 diabetes mellitus. *Am. J. Clin. Nutr.* 90, 468–476. doi: 10.3945/ajcn.2008.27371

Pérez, P., and De Los Campos, G. (2014). Genome-wide regression and prediction with the BGLR statistical package. *Genetics* 198, 483–495. doi: 10.1534/genetics.114.164442

Raclot, T., Groscolas, R., Langin, D., and Ferré, P. (1997). Site-specific regulation of gene expression by n-3 polyunsaturated fatty acids in rat white adipose tissues. *J. Lipid Res.* 38, 1963–1972. doi: 10.1016/s0022-2275(20)37127-3

Realini, C. E., Duran-Montgé, P., Lizardo, R., Gispert, M., Oliver, M. A., and Esteve-Garcia, E. (2010). Effect of source of dietary fat on pig performance, carcass characteristics and carcass fat content, distribution and fatty acid composition. *Meat. Sci.* 85, 606–612. doi: 10.1016/j.meatsci.2010.03.011

Rohart, F., Gautier, B., Singh, A., and Lê Cao, K.-A. (2017). mixOmics: An R package for 'omics feature selection and multiple data integration. *PloS Comput. Biol.* 13, e1005752. doi: 10.1371/journal.pcbi.1005752

Rydén, M., and Arner, P. (2017). Subcutaneous adipocyte lipolysis contributes to circulating lipid levels. *Arterioscler. Thromb. Vasc. Biol.* 37, 1782–1787. doi: 10.1161/ATVBAHA.117.309759

Saadatian-Elahi, M., Slimani, N., Chajès, V., Jenab, M., Goudable, J., Biessy, C., et al. (2009). Plasma phospholipid fatty acid profiles and their association with food intakes: results from a cross-sectional study within the European Prospective Investigation into Cancer and Nutrition. *Am. J. Clin. Nutr.* 89, 331–346. doi: 10.3945/ajcn.2008.26834

Sarmiento-Garcia, A., and Vieira-Aller, C. (2023). Improving fatty acid profile in native breed pigs using dietary strategies: a review. *Anim. (Basel).* 13, 1696. doi: 10.3390/ani13101696

Segura, J., and Lopez-Bote, C. J. (2014). A laboratory efficient method for intramuscular fat analysis. *Food Chem.* 145, 821–825. doi: 10.1016/j.foodchem.2013.08.131

Senanayake, V. K., Pu, S., Jenkins, D. A., Lamarche, B., Kris-Etherton, P. M., West, S. G., et al. (2014). Plasma fatty acid changes following consumption of dietary oils containing n-3, n-6, and n-9 fatty acids at different proportions: preliminary findings of the Canola Oil Multicenter Intervention Trial (COMIT). *Trials* 15, 136. doi: 10.1186/1745-6215-15-136

Sessler, A. M., and Ntambi, J. M. (1998). Polyunsaturated fatty acid regulation of gene expression. *J. Nutr.* 128, 923–926. doi: 10.1093/jn/128.6.923

Shannon, P., Markiel, A., Ozier, O., Baliga, N. S., Wang, J. T., Ramage, D., et al. (2003). Cytoscape: A software environment for integrated models of biomolecular interaction networks. *Genome Res.* 13, 2498–2504. doi: 10.1101/gr.1239303

Singh, A., Shannon, C. P., Gautier, B., Rohart, F., Vacher, M., Tebbutt, S. J., et al. (2019). DIABLO: an integrative approach for identifying key molecular drivers from multi-omics assays. *Bioinformatics* 35, 3055–3062. doi: 10.1093/bioinformatics/bty1054

Song, C. H., Oh, S. M., Lee, S., Choi, Y., Kim, J. D., J-ang, A., et al. (2020). The ratio of dietary n-3 polyunsaturated fatty acids influences the fat composition and lipogenic enzyme activity in adipose tissue of growing pigs. *Food Sci. Anim. Resour.* 40, 242–253. doi: 10.5851/kosfa.2020.e8

Stegemann, C., Pechlaner, R., Willeit, P., Langley, S. R., Mangino, M., Mayr, U., et al. (2014). Lipidomics profiling and risk of cardiovascular disease in the prospective population-based Bruneck study. *Circulation* 129, 1821–1831. doi: 10.1161/CIRCULATIONAHA.113.002500

Surette, M. E., Whelan, J., Broughton, K. S., and Kinsella, J. E. (1992). Evidence for mechanisms of the hypotriglyceridemic effect of n – 3 polyunsaturated fatty acids. *Biochim. Biophys. Acta* 1126, 199–205. doi: 10.1016/0005-2760(92)90291-3

Tian, M., Hao, F., Jin, X., Sun, X., Jiang, Y., Wang, Y., et al. (2021). ACLY ubiquitination by CUL3-KLHL25 induces the reprogramming of fatty acid metabolism to facilitate iTreg differentiation. *Elife* 7, e62394. doi: 10.7554/eLife.62394

Wang, X., Tsai, T., Deng, F., Wei, X., Chai, J., Knapp, J., et al. (2019). Longitudinal investigation of the swine gut microbiome from birth to market reveals stage and growth performance associated bacteria. *Microbiome* 7, 109. doi: 10.1186/s40168-019-0721-7

Warensjö, E., Öhrvall, M., and Vessby, B. (2006). Fatty acid composition and estimated desaturase activities are associated with obesity and lifestyle variables in men and women. *Nutr. Metab. Cardiovasc. Dis.* 16, 128–136. doi: 10.1016/j.numecd.2005.06.001

Warensjö, E., Risérus, U., and Vessby, B. (2005). Fatty acid composition of serum lipids predicts the development of the metabolic syndrome in men. *Diabetologia* 48, 1999–2005. doi: 10.1007/s00125-005-1897-x

Warensjö, E., Rosell, M., Hellenius, M. L., Vessby, B., De Faire, U., and Risérus, U. (2009). Associations between estimated fatty acid desaturase activities in serum lipids and adipose tissue in humans: links to obesity and insulin resistance. *Lipids Health Dis.* 27, 37. doi: 10.1186/1476-511X-8-37

Willumsen, N., Skorve, J., Hexeberg, S., Rustan, A. C., and Berge, R. K. (1993). The hypotriglyceridemic effect of eicosapentaenoic acid in rats is reflected in increased mitochondrial fatty acid oxidation followed by diminished lipogenesis. *Lipids* 28, 683–690. doi: 10.1007/BF02535987

Wood, J. D., Enser, M., Fisher, A. V., Nute, G. R., Richardson, R. I., and Sheard, P. R. (1999). Manipulating meat quality and composition. *Proc. Nutr. Soc.* 58, 363–370. doi: 10.1017/S0029665199000488

Yang, K. X., Ma, J. W., Guo, Y. M., Guo, T. F., Zhao, Y. G., Ding, N. S., et al. (2010). Correlations between fat depot traits and fatty acid composition in abdominal subcutaneous adipose tissue and longissimus muscle: Results from a White Duroc × Erhualian intercross F2 population. *J. Anim. Sci.* 88, 3538–3545. doi: 10.2527/jas.2009-2602

Yi, W., Huang, Q., Wang, Y., and Shan, T. (2023). Lipo-nutritional quality of pork: The lipid composition, regulation, and molecular mechanisms of fatty acid deposition. *Anim. Nutr.* 13, 373–385. doi: 10.1016/j.aninu.2023.03.001

Zhou, X., Zhu, X., Li, C., Li, Y., Ye, Z., Shapiro, V. S., et al. (2021). Stearoyl-CoA desaturase-mediated monounsaturated fatty acid availability supports humoral immunity. *Cell Rep.* 34, 108601. doi: 10.1016/j.celrep.2020.108601

Zhou, X., Zhu, X., and Zeng, H. (2023). Fatty acid metabolism in adaptive immunity. *FEBS J.* 290, 584–599. doi: 10.1111/febs.16296